ACS APPLIED MATERIALS & INTERFACES

Research Article

www.acsami.org

Tracking Structural Changes in Lipid-based Multicomponent Food Materials due to Oil Migration by Microfocus Small-Angle X-ray Scattering

Svenja K. Reinke,*[,†] Stephan V. Roth,[‡] Gonzalo Santoro,[‡,⊥] Josélio Vieira,[§] Stefan Heinrich,[†] and Stefan Palzer[∥]

[†]Institute of Solids Process Engineering and Particle Technology, Denickestr. 15, 21075 Hamburg, Germany

[‡]Photon Science, DESY, Notkestr. 85, 22607 Hamburg, Germany

[§]Nestlé Product Technology Centre York, P.O. Box 204, Haxby Road, York YO91 1XY, England, United Kingdom

[∥]Nestlé SA, Avenue Nestlé 55, 1800 Vevey, Switzerland

ABSTRACT: One of the major problems in the confectionery industry is chocolate fat blooming, that is, the formation of white defects on the chocolate surface due to fat crystals. Nevertheless, the mechanism responsible for the formation of chocolate fat blooming is not fully understood yet. Chocolate blooming is often related to the migration of lipids to the surface followed by subsequent recrystallization. Here, the migration pathway of oil into a cocoa butter matrix with different dispersed particles was investigated by employing microfocus small-angle X-ray scattering and contact angle measurements. Our results showed that the chocolate powders get wet by the oil during the migration process and that the oil is migrating into the pores within seconds. Subsequently, cocoa butter is dissolved by the oil, and thus, its characteristic crystalline structure is lost. The chemical process provoked by the dissolution is also reflected by microscopical changes of the surface morphology of chocolate model samples after several hours from the addition of oil to the sample. Finally, the surface morphology was investigated before and after oil droplet exposure and compared to that of water exposure, whereby water seems to physically migrate through the particles, namely cocoa powder, sucrose, and milk powder, which dissolve in the presence of water.

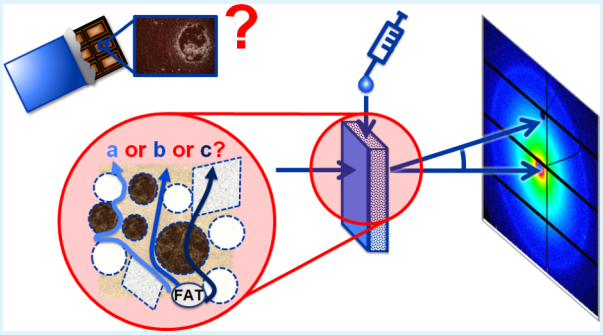

KEYWORDS: *μSAXS, synchrotron, migration, chocolate, microstructure*

INTRODUCTION

Controlling molecular migration in food products is of high relevance for the food industry because this process leads to major quality issues such as chocolate blooming or softening of bakery products.[1,2] Chocolate blooming consists of the formation of visible white spots or a greyish haze on the chocolate surface, which results in consumer complaints and large sales losses for the food industry. Many food products, such as chocolate, confectioneries, and bakery products, are multicomponent materials consisting of microscopic particles embedded in a continuous matrix.[1,3] Aguilera et al.[2] have proposed to consider chocolate as a particulate medium consisting of an assembly of fat-coated particles (cocoa solids, sucrose, and, in the case of milk chocolate, milk powder particles) embedded in a continuous fat phase (Figure 1). Often, an emulsifier, which surrounds the solid particles, is added to adjust the material rheology.[4] Thus, due to the multicomponent nature of chocolate, the molecular migration may take place through the continuous matrix phase, through a continuous network of particles, or through the interface between the matrix and the particles (Figure 1).

Moreover, the migration through the fat phase could be diffusion-based or due to a convective flow, for example, through crevices in the solid fat matrix. Both transport processes are extensively discussed in the literature.[1−3,5,6] However, the exact mechanism and the preferential migration pathway through chocolate is still not well understood.[1,2,4]

The main fat in chocolate is cocoa butter (CB), which is mainly comprised of three key triglycerides (1,3-dipalmitoyl-2-oleoyl-glycerol (POP), 1,3-distearoyl-2-oleoylglycerol (SOS), and palmitoyl-stearoyl-2-oleoyl-glycerol (POS))[4,7] and is partly liquid and partly solid at room temperature.[1] The solid fat content depends on the crystalline structure, triglyceride composition, and storage conditions of the CB.

From a crystallographic point of view, CB presents six known polymorphs,[4,7] which are denoted either using Roman numerals (I−VI) or using the crystallographic nomenclature (γ, α, β_2', β_1', β_2, β_1). Both nomenclatures are evenly used in

Received: March 9, 2015
Accepted: April 20, 2015
Published: April 20, 2015

DOI: 10.1021/acsami.5b02092
ACS Appl. Mater. Interfaces 2015, 7, 9929−9936

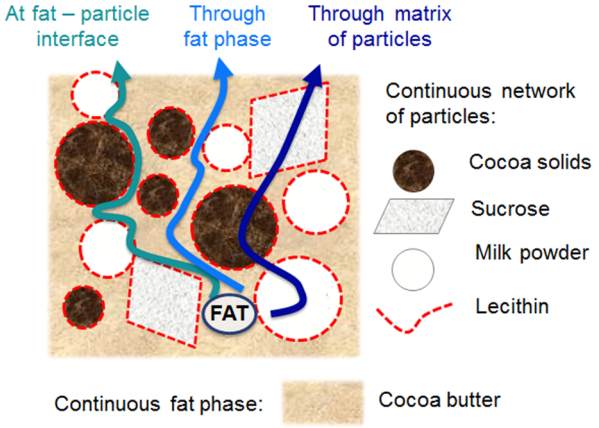

Figure 1. Possible lipid migration pathways in chocolate, a multicomponent material.

the literature and are interchangeable. Here, we will use the Roman numerals to denote the CB polymorphs.

The crystalline stability of CB increases from form I to VI, and form V is the main crystalline form in chocolate. This polymorph presents the final desirable thermal and mechanical properties and gives rise to optimal chocolate appearance, and thus, it is preferred in consumer products. The formation of fat bloom has been associated with a crystalline transformation in the CB from form V to VI, degrading the appearance of chocolate products. In addition, it has been reported that several CB polymorphs can coexist.[8]

Fat and oil migration in chocolate have been mainly investigated on a macroscopic level employing the so-called washer test, whereby migrant and material are brought into contact and stored under controlled conditions. Afterwards, the sample is analyzed at defined times, wherefore destruction of the sample is necessary. Thereby, triglyceride distribution using, for example, gas or liquid chromatography, analysis of iodine index or isooleic acid content, solid fat content (NMR/MR), and gravimetric analyses are commonly used to detect and quantify migration.[1,5,9] Furthermore, nondestructive magnetic resonance imaging (MRI)[3] has provided information about the migration process on a macroscopic level and tracer components have been employed to follow the migration process as well.[1,10,11]

Here, oil migration through multicomponent food materials was investigated using synchrotron microfocus small-angle X-ray scattering (μSAXS), which reveals structural changes in the range of a few nanometers up to 125 nm, to gain further insights into microscopic and molecular processes during oil migration into chocolate. A better understanding of these processes is essential to decipher the preferential migration pathway, which cannot be macroscopically addressed given the microscopic nature of chocolate. Moreover, using a non-destructive method, we can analyze the sample continually over time.

X-ray scattering has already been applied to investigate the structure of complex food materials, such as hen-egg yolk, an oil-in-water emulsion with lipids and proteins.[12] Dynamic processes in food materials, such as diffusion of a proteinase on a casein film, have also been analyzed with X-ray scattering techniques.[13] In this study, three different powder components (cocoa solids, skimmed milk powder, and sucrose) surrounded by CB have been investigated. A new in situ and nondestructive methodology has been established to evaluate structural changes due to oil migration. Additionally, wetting and migration behavior was investigated by contact angle measurements using the sessile drop protocol.

MATERIALS AND METHODS

Natural cocoa powder (fat content: 11 ± 1%) and medium heated skimmed milk powder were used as powder materials. Furthermore, refiner flakes with 27% cocoa butter and skimmed milk powder (particle size ∼15 μm) were produced. Additionally, sucrose powder was refined with 23% CB obtaining CB coated flakes with a particle size of approximately 20 μm. Powder materials and CB were provided by Nestlé Product Technology Center (PTC; York, U.K.). Powder samples were stored under ambient conditions.

Furthermore, four different chocolate model samples, namely, a pure CB (Nestlé PTC) bulk sample, CB/cocoa powder (Bensdorp, Germany), CB/skimmed milk powder (Nestlé PTC), and CB/sucrose (Sweet Family Nordzucker Puderzucker, Germany) were prepared and tempered as follows. First, CB was melted at 50 °C for at least 1 h on a stirred hot plate, and then the powder (cocoa, milk, or sucrose) was added in a 4:1 volume concentration (volume powder/volume cocoa butter) and further stirred at 31.5 °C and at 100 rpm for 5 min. Then, 1 wt % of cocoa butter powder seeds in the form V crystalline structure were added, and the suspension was stirred for 10 more minutes. Subsequently, the resulting mass was molded and cooled at 5 °C overnight.

Food retail sunflower oil (VITA D'OR, Brökelmann & Co. Oelmühle GmbH & Co. KG, Germany) with 92 wt % fat (10 wt % saturated fatty acids, 29 wt % monounsaturated, and 53 wt % polyunsaturated (omega-6-linoleic acid)) was used as oil migrant for both μSAXS and contact angle experiments.

Scanning electron microscopy (SEM) was used to image the powder samples using a Zeiss Supra 55 VP FEG-REM. The aperture size was 10 μm, and the secondary electrons were detected. The voltage was adjusted from 1 to 3 kV according to optimum image quality.

The contact angle was measured employing the sessile drop protocol. Therefore, a droplet with a volume of 0.7 ± 0.1 μL was deposited on the surface of the chocolate model samples with a pipet. Images of the droplet were acquired with a high-speed camera (Serie NX-S2) connected to a microscope objective from OPTEM ZOM 125. Recording was realized with the software "Motion Studio" (Integrated Design Tools, Inc., Tallahassee, FL). The images were analyzed with a drop shape plugin in ImageJ.[14]

Differential scanning calorimetry (DSC) measurements have been conducted with a NETZSCH DSC 204 F1 Phoenix. The samples (13.5 ± 1.0 mg) were first cooled to 15 °C and subsequently heated up from 15 to 50 °C at 1 K/min. The enthalpy of melting ΔH was determined by integration of the melting peak from 22.5 to 35 °C and a linear baseline with Origin (OriginLab, Northampton, MA).

μSAXS measurements were performed at the MiNaXS/P03-beamline of the PETRA III storage ring at DESY (Deutsches Elektronen Synchrotron).[15−17] A beamsize of (31 × 22) μm^2 was used at a wavelength of λ = 1.090 ± 0.005 Å. The sample to detector distance was set at (3651 ± 1) mm. A 1 M Pilatus detector (Dectris Ltd., Switzerland) with a pixel size of 172 × 172 μm^2 was used. The powder samples were placed in a 1 mm thick sample cell made of Kapton foil (thickness: 76 μm). A sample volume of 0.12 ± 0.01 mm^3 was used.

Instead of single X-ray exposure at a fixed position, a vertical scan with 61 points (step size, 100 μm) was performed for each time step to account for effects due to sample heterogeneity (Figure 2). By using a small microfocus beam in a scan mode with the given experimental procedure beam damage of the sample is avoided and a good signal-to-noise ratio is achieved. A preliminary test proved that the structure is not modified due to beam exposure for 1 s. In addition, by using a microfocused beam, truly statistical values are extracted, and deviations from the mean values can be evaluated, rather than only average macroscopic values.

DOI: 10.1021/acsami.5b02092
ACS Appl. Mater. Interfaces 2015, 7, 9929−9936

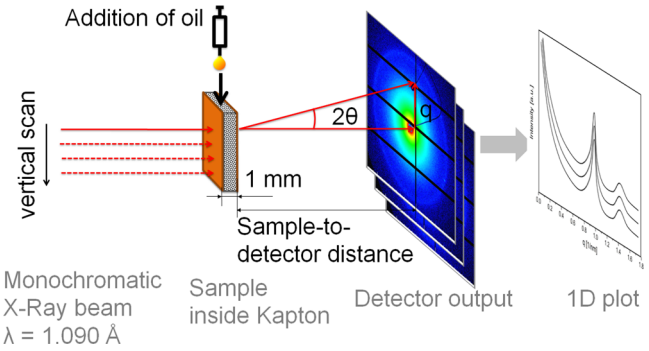

Figure 2. Sketch of the experimental μSAXS setup: X-ray beam going through a sample and leaving a scattering pattern as detector output, which can be transferred into a 1D plot. A vertical scan with 61 images with step sizes of 0.1 mm was done for each sample at each time step.

A first scan was performed before the addition of oil. Then, approximately 10 μL of oil was deposited through an upper aperture in the sample cell, and a second vertical scan was performed. A vertical scan was then repeated 5, 10, and 30 min after oil addition, and, for selected samples, additional scans after 1 h, 2 h, 5 h, and 1 day were realized. To avoid beam-induced effects, we set the exposure time to 1 s, and a horizontal shift of 500 μm was realized between every vertical scan.

For each vertical scan, the 61 scattering patterns were summed. A mask was applied to account for the intermodular detector gaps, and the beam stop (used to prevent the detector from oversaturation due to the high X-ray intensity) and standard normalization were performed. Afterwards, the 2D scattering patterns were transformed into 1D data plots by radial integration using the DPDAK software package.[18]

The scattering peaks were fitted using the DPDAK software with a pseudo-Voigt profile combined with a linear background. On the other hand, the scattering power (k) is the total scattered integral intensity, which depends on the electron density difference ($\Delta\rho$), the volume fraction (ν) and the irradiated volume (V):

$$k = \int I(q)d^3q = (\Delta\rho)^2\nu(1-\nu)V \quad (1)$$

The equation applies for nonparticulate two-phase systems.[19]

The scattering power (k^*) of the measured 1D data system has been calculated in Origin (OriginLab, Northampton, MA) according to

$$k^* = \int_{q_{min}=0.05\mathrm{nm}^{-1}}^{q_{max}=1.71\mathrm{nm}^{-1}} I(q)d^3q \quad (2)$$

For powders having highly ordered structures, the peak intensity and shoulder intensity, respectively, were calculated with

$$k_{peak} = \int I_{fit}(q)d^3q - \int I_{baseline}(q)d^3q \quad (3)$$

The difference of the total scattering power and all peak intensities is then:

$$\Delta k = k^* - \sum k_{peak} \quad (4)$$

RESULTS AND DISCUSSION

Five different samples were investigated by μSAXS. Overall, three q-regions corresponding to ordered structures can be identified in the μSAXS patterns of the dry powders before migration of oil started (Figure 3, Table 1).

The peaks at q = 0.97 nm^{-1} and q = 1.39 nm^{-1} are the characteristic peaks of CB forms V and IV, respectively (d-spacings of 6.50 and 4.50 nm). Wille and Lutton[20] and Chapman et al.[21] reported a d-spacing for CB in form IV ranging from 4.50 to 4.90 nm, for form V from 6.41 to 6.60 nm and for CB in form VI from 6.3 to 6.38 nm.[20,21] Only the CB IV and V polymorphs were observed in the pure CB and in the CB with powders (sucrose and skimmed milk).

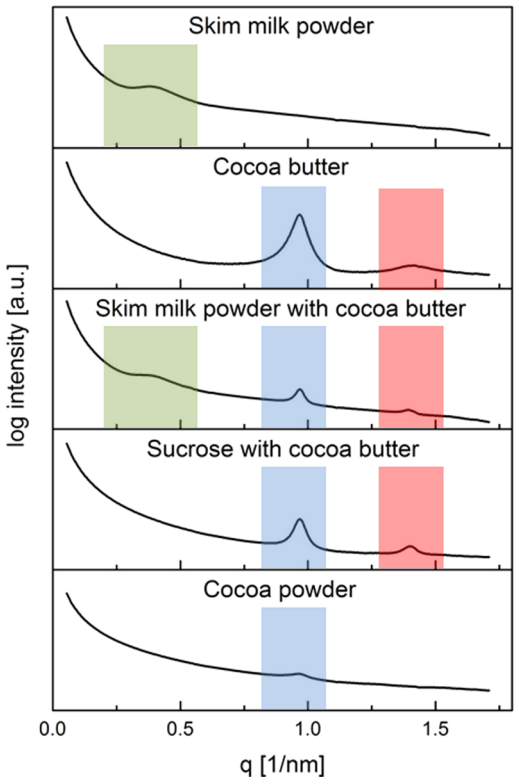

Figure 3. Scattering curves of dry powders, sum of vertical scan (images 1−61).

Table 1. Peak Center of Investigated Dry Powders and Corresponding d-Spacing

material	peak center (1/nm)	d-spacing (nm)	assignment[a]
cocoa butter (CB)	$0.97^{+\ 0.00}_{-\ 0.01}$	6.50 ± 0.01	CB, form V
	1.41 ± 0.02	4.46 ± 0.03	CB, form IV
cocoa powder	0.97 ± 0.01	6.49 ± 0.07	CB, form V
skimmed milk powder	0.40 ± 0.00	$15.84^{+\ 0.01}_{-\ 0.12}$	
skimmed milk powder with CB	$0.97^{+\ 0.00}_{-\ 0.01}$	$6.51^{+\ 0.06}_{-\ 0.01}$	CB, form V
	1.39 ± 0.00	4.51 ± 0.01	CB, form IV
	0.39 ± 0.00	$16.25^{+\ 0.01}_{-\ 0.04}$	
sucrose with CB	0.97 ± 0.00	6.50 ± 0.00	CB, form V
	1.40 ± 0.00	$4.49^{+\ 0.00}_{-\ 0.01}$	CB, form IV

[a]According to Wille and Lutton[20] and Chapman et al.[21]

The shoulder at a q value of around 0.4 nm^{-1} corresponds to a d-spacing of 15.84 nm (Figure 3, Table 1) and is well-known for milk products as being characteristic of the supramolecular structure of casein, which is present in skimmed milk powder. According to Gebhardt et al.,[22,23] casein micelles are spherical protein aggregates with diameters of 50−500 nm. However, the exact internal structure of casein micelles is still not fully understood.[13,22,23] On the other hand, Holt et al.[24] and Shukla et al.[25] observed a shoulder near q = 0.35 nm^{-1}, which was attributed to calcium phosphate nanoclusters. McMahon and Oommen[26] have proposed a casein structure model, which

DOI: 10.1021/acsami.5b02092
ACS Appl. Mater. Interfaces 2015, 7, 9929−9936

does not present a classical micellar structure, but the casein form linear and branched chains being interlocked by the calcium phosphate nanoclusters that are stabilized by the casein. Gebhardt et al.[22] measured casein films and found shoulders at q = 0.03 nm^{-1} (attributed to the size of casein micelles), at q = 0.1 nm^{-1} (arising from micellar substructures, so-called mini micelles), and at q = 1 nm^{-1} (attributed to the colloidal calcium phosphate). Gebhardt et al. found that the size of the mini micelles can vary from 10 to 20 nm with increasing calcium content, and they reported a q value of q = 0.3 nm^{-1}, attributed to casein submicelles, which was less pronounced than the shoulders at q = 0.025 and 1 nm^{-1}.[22,27] In our case, the results do not show pronounced peaks for skim milk powder besides that at q = 0.4 nm^{-1}, characteristic of the supramolecular structure of casein, as already mentioned (Figure 3).

The DSC measurements of selected samples (Figure 4, Table 2) show a prominent melting peak with an onset temperature

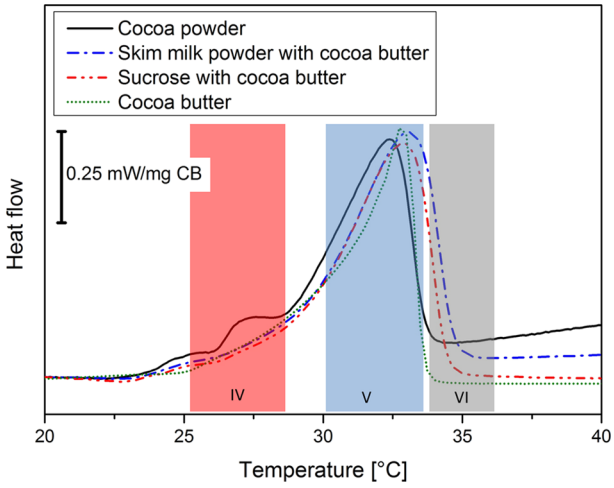

Figure 4. Differential scanning calorimetric measurement of selected samples. The melting temperature ranges for different CB polymorphs are indicated in the figure.

Table 2. Melting Temperatures and Melting Enthalpies of Cocoa Butter in Powder Samples Extracted from DSC

material	onset temp (°C)	peak center (°C)	enthalpy of melting (J/mg CB)
cocoa butter (CB)	25.0	32.7	128.7
cocoa powder	22.9	32.4	127.2
skimmed milk powder with CB	22.6	33.1	152.3
sucrose with CB	22.6	32.9	153.2

of 22.9 °C and a maximum at 32.4 °C for cocoa powder. The onset temperature for the refiner flakes with CB and sucrose (maximum at 32.9 °C) and for the refiner flakes of skimmed milk powder with CB (maximum at 33.1 °C) is 22.6 °C. The cocoa butter melting peak starts at 25.0 °C and has its maximum at 32.7 °C.

In CB−powder mixture, the most prominent peak is the CB form V peak at q = 0.97 nm^{-1}, indicating preponderance over form IV. The fat phase was not subjected to any thermal treatment and was held in its original structure. Forms IV and V are both stable at room temperature, but form V is thermodynamically more favorable and, therefore, transforms into this polymorph.[28] The form IV peak for cocoa powder is not visible in the μSAXS measurements even though a small but identifiable peak in the form IV polymorph can be observed in the DSC results for cocoa powder (Figure 4).

The melting temperature range for CB form IV ranges from 25.6[21] to 27.5 °C,[20] whereas the form V melting temperature varies from 30.8[21] to 33.87 °C,[20] and form VI varies from 32.3[21] to 36.3 °C.[20] The CB form IV crystals cannot be clearly identified in the DSC measurements of the CB-powder mixtures because they are probably convoluted with the form V melting peak. As mentioned in literature,[20,21,28] CB has a broad range of melting temperatures, which is dependent on the exact composition and thermal history. The melting enthalpies (Table 2) of pure CB and cocoa powder are 128.7 and 127.2 J/mg CB, respectively, which are lower than those of the refiner flakes, 152.3 and 153.2 J/mg CB for the skimmed milk powder with CB and sucrose with CB, respectively. Thus, the crystal content and, consequently, solid fat content of CB is higher for the refiner flakes. The CB and cocoa powder are in their natural states, whereas the refiner flakes were melted and solidified during production process. The sucrose and skimmed milk powder particles might thereby have acted as heterogeneous nucleation agents for crystallization of the CB matrix leading to higher crystal content.

Apart from the identification of CB polymorphs, the μSAXS data were also employed to gain a deeper insight into the polymorph distribution, as can clearly be observed in Figure 5.

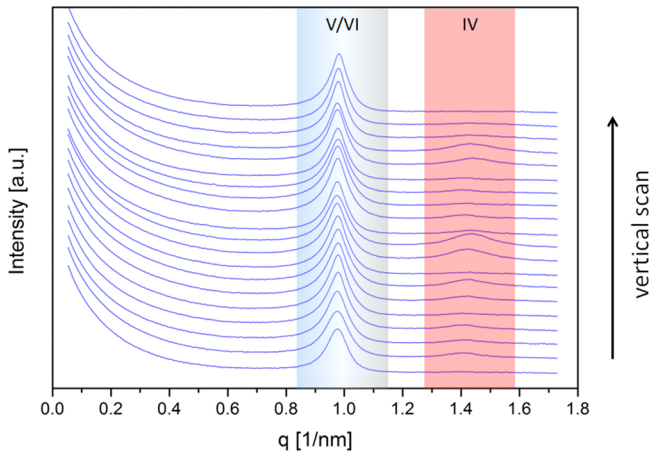

Figure 5. 1D scattering patterns of CB dry powder. Scattering patterns of positions 1−20 in the vertical scan. The q ranges of form IV and V/VI are indicated in the figure.

CB form V is predominant in every measured point, whereas the crystalline CB polymorphic form IV is heterogeneously distributed in the sample, as revealed by the fact that the form IV peak at 1.39 nm^{-1} is not present at every spatial point (Figure 5). Thus, the μSAXS patterns clearly demonstrate that the CB sample possess crystal grains in different polymorphic forms. The distance between the X-ray beam center of two adjacent scattering points is 100 μm with a beamsize of 22 μm in the vertical direction. Two adjacent points with CB form IV identify grain sizes of up to 122 μm. In contrast, the sucrose with CB sample showed in every measured spatial point equally distributed polymorphic forms IV and V with smaller peak width for the IV peak. The skimmed milk powder with CB showed identifiable CB form IV peaks in around 75% of the investigated spatial points.

DOI: 10.1021/acsami.5b02092
ACS Appl. Mater. Interfaces 2015, 7, 9929−9936

For the study of oil migration, the complete set of 61 images of every vertical scan has been summed to get representative results of the heterogeneous sample at each defined oil migration time. Then, the difference in total scattering power has been calculated at each defined time.

Before the addition of oil, the difference in total scattering power (Δk; Figure 6) is predominantly influenced by the

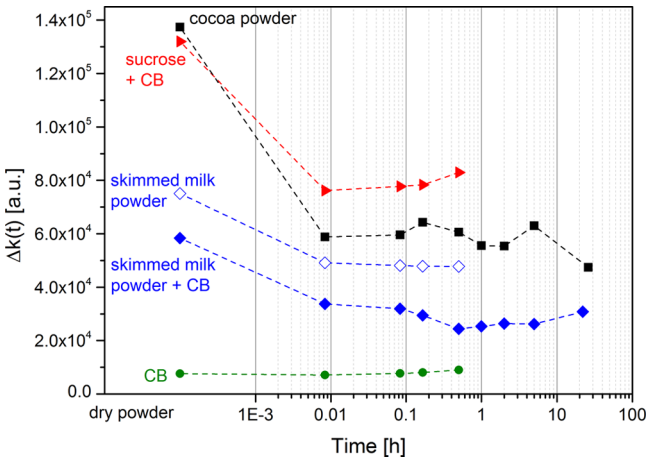

Figure 6. Difference of total scattering power of different powders in dependence of migration time; sunflower oil migration into cocoa butter (CB, --●--), skimmed milk powder (--◊--), skimmed milk powder refined with 27% cocoa butter (--♦--), sucrose refined with 23% cocoa butter (--▶--), and cocoa powder (--■--).

porous structure of the powder samples, leading to significant scattering in the measured range. The strong scattering for all powders reveals the presence of pores in the range of 3.5−125 nm.[19,29] The porous structure of the powders is also visible in SEM images (Figure 7).

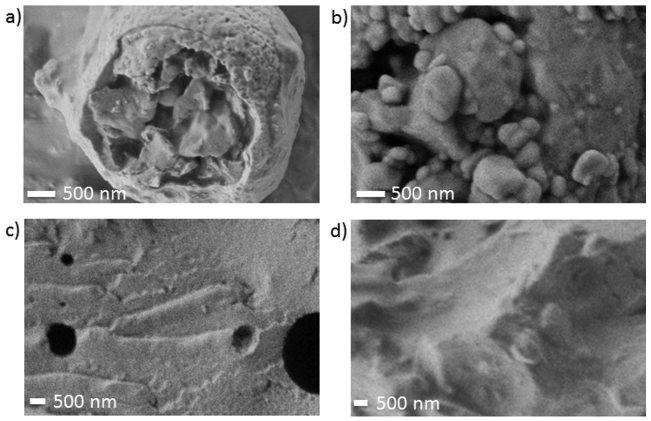

Figure 7. SEM images of (a) cocoa powder, (b) sucrose refined with cocoa butter, (c) skimmed milk powder, and (d) skimmed milk powder refined with cocoa butter.

Pure CB presents lower Δk values due to its less porous structure as compared to the other samples, whereas in the case of skimmed milk powder, it can be seen that Δk decreases when the powder is coated with cocoa butter, which is probably due to the CB coating blocking the pores. This point has been further confirmed by SEM (Figure 7).

On the other hand, cocoa powder is a highly porous network of cocoa solid material coated with CB. The surface of a cocoa powder particle has many pores in the μSAXS range used here (3.5−125 nm), and the entire structure is highly fractal. Skimmed milk powder has pores in the measured range as well; however, it has fewer pores compared to cocoa powder, which explains the lower Δk.

Due to the addition of oil, Δk decreases for every powder sample but remains almost constant for the CB sample (Figure 6). The most significant decrease in Δk takes place in the first minutes and further decrease slows down with time. This can be explained considering a change in X-ray scattering contrast due to oil migration, because the contrast is different between the solid material and air as compared to the difference between powder material and oil. According to the equation introduced by Porod,[19] a change in Δk occurs whenever a change in scattering contrast takes place, assuming a constant volume of scattering material. These results reveal that the oil migrates into the pores within the first minutes. The Δk value of CB does not change significantly because, presumably, there are no or not many porous structures within the detection range (3.5−125 nm), and therefore, no significant change in scattering contrast takes place indicating that oil migration occurs predominantly through the porous structures in the first few minutes.

Besides the aforementioned important results, the integral intensity of the crystalline peak associated with CB form V (q = 0.97 nm^{-1}) decreases gradually with time (Figure 8). Unfortunately, due to the weak signal of the peak associated with form IV, the expected changes in the intensity of this peak could not be followed.

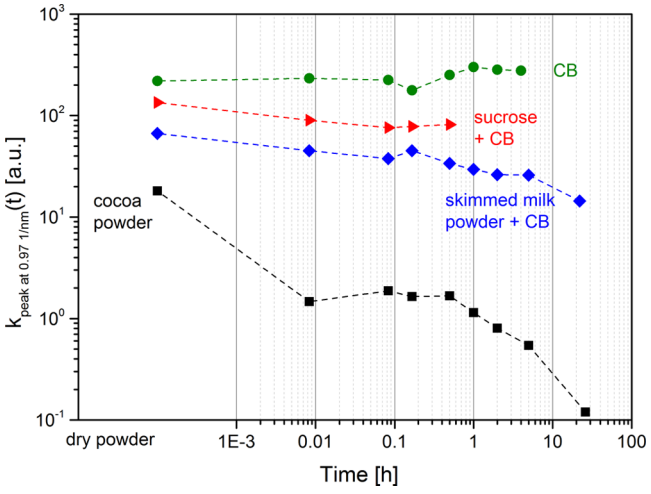

Figure 8. Peak intensity of cocoa butter peak (form V/VI) at different oil exposure; sunflower oil migration into cocoa butter (CB, --●--), skimmed milk powder refined with 27% cocoa butter (--♦--), sucrose refined with 23% cocoa butter (--▶--), and cocoa powder (--■--).

The decrease in the CB form V peak implies that oil migration is provoking, for longer times, a loss of the crystalline structure. The oil migration into the CB fat phase might lead to a mixture of these two lipid materials, hence the solid fat content decreases. Zeng et al.[30] measured a solid fat decrease from 80 to 20% at 24 °C when the concentration of almond oil is increased to 50% in a mixture of CB and almond oil.[4,30] Furthermore, solution of the solid CB phase in the oil may occur.[31,32] The peak of pure CB does not significantly decrease within 5 h, which might be due to little surface area available for fat dissolution by the migrated oil in case of pure CB. In

DOI: 10.1021/acsami.5b02092
ACS Appl. Mater. Interfaces 2015, 7, 9929−9936

contrast, the cocoa powder and refiner flakes samples present higher porosity (Figure 6). Thus, higher surface area is available, and the dissolution process is accelerated.

The analysis of the single images for all samples revealed that structural changes occurred in the same magnitude over all 61 points of the vertical scan, ensuring that mean values are representative of the system. In addition, this shows that the oil was equally distributed over the scanned area during the experiment.

On the macroscopic scale, the slow solution of the solid CB in model chocolate samples has been investigated by contact angle measurements employing the sessile droplet protocol. The volume of the oil droplet on the surface of the chocolate model system remains constant within the first 12.5 min. Hence, no detectable oil migration or absorption took place within the detection limits (Figure 9).[33] However, there is a slight decrease in the contact angle due to further spreading on the sample within the first minutes (Figure 10).

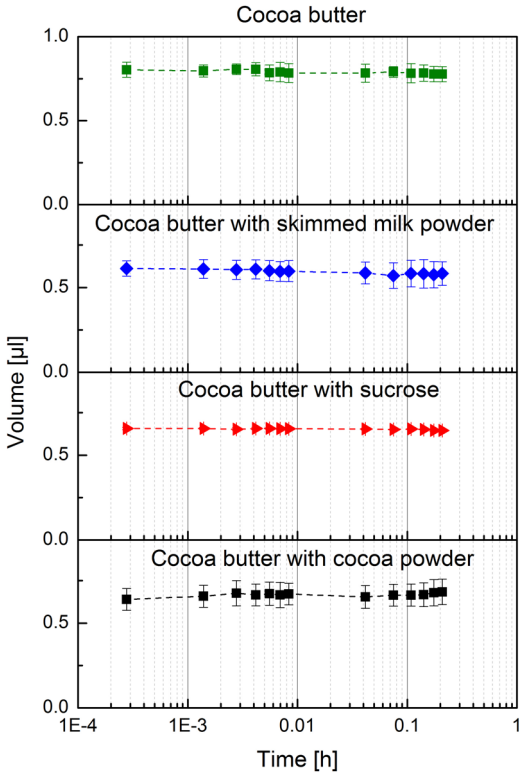

Figure 9. Volume of sessile drop of sunflower oil on surface of chocolate model systems.

No significant influence of the embedded particles on the wetting and migration of sessile oil droplets was detected. The contact angle starts at a value slightly larger in the case of skimmed milk powder as compared to the other samples and then decreases slightly faster. This behavior is characteristic of rougher surfaces, which might be due to the embedded particle phase. On the other hand, the starting contact angle value for sucrose is slightly lower compared to the other materials, which is due to the hydrophilic nature of sugar.

To gain some insight into surface changes due to the presence of oil, we imaged the surface of chocolate model systems with a light microscope before and after 5 h from sessile drop exposure when the droplet vanished completely (Figure 11).

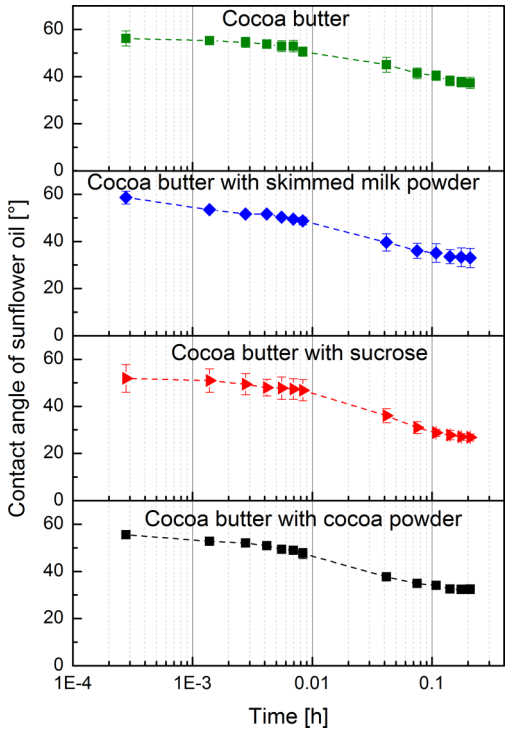

Figure 10. Contact angle of sessile drop of sunflower oil on surface of chocolate model systems.

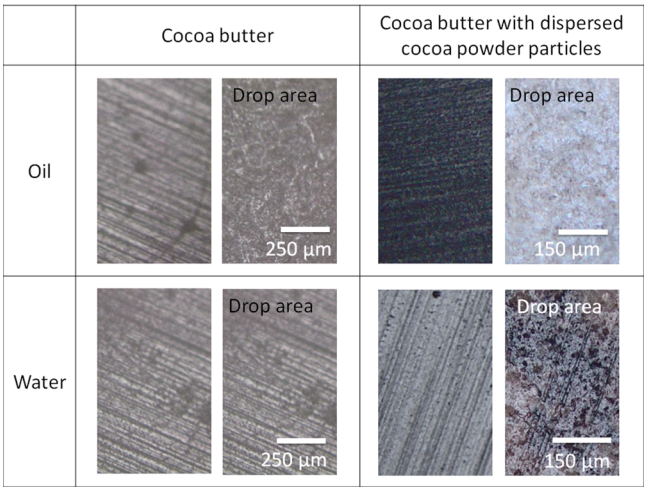

Figure 11. Microscope images of sample surfaces before and after drop exposure.

The regular lined original shaped surface is due to the mold. When exposed to oil, the surface of both chocolate model samples exhibited a significant morphological change, macroscopically reflecting the oil migration through the CB in the long term. Just for comparison, the experiments were repeated with water. In this case, only particle swelling was observed but no morphological changes associated with liquid migration are observed.

CONCLUSION

By employing synchrotron μSAXS and contact angle measurements, we investigated the pathway of oil migration in multicomponent food materials containing cocoa butter. The results suggest that oil is first migrating through pores and

DOI: 10.1021/acsami.5b02092
ACS Appl. Mater. Interfaces 2015, 7, 9929−9936

cracks in the solid structure probably driven by capillary pressure. Subsequently, chemical migration through the fat phase takes place, inducing softening and partial dissolution of the crystalline cocoa butter.

Thus, the mechanism for lipid migration in chocolates probably involves both capillary rise, to be considered as the dominant mechanism in the short term, and molecular migration. Thereby, wettability of the solid system impacts the progress of liquid in the capillaries. However, the results also suggest that wetting is not the only mechanism. Considering longer observation times, chemical migration of lipids significantly contribute to the overall process. Because the most probable migration pathway due to wetting occurs through the material porous structure, this process could be prevented by a reduction of porosity and a minimization of defects in the chocolate matrix, which might act as pathways. On the other hand, the effect of dissolution and chemical migration could be minimized by ensuring a reduced content of noncrystallized liquid cocoa butter. Overall, our results allow to address a major problem in the confectionery industry, namely, fat blooming of chocolate.

AUTHOR INFORMATION

Corresponding Author

*E-mail: svenja.reinke@tuhh.de.

Present Address

[⊥]Instituto de Ciencia de Materiales de Madrid, CSIC, Sor Juana Inés de la Cruz 3, Cantoblanco, 28049 Madrid, Spain.

Author Contributions

The manuscript was written through contributions of all authors. All authors have given approval to the final version of the manuscript.

Notes

The authors declare no competing financial interest.

ACKNOWLEDGMENTS

The authors thank John Rasburn (former Nestlé PTC, York) for his guidance during planning and analysis of the μSAXS experiment. Parts of this research were carried out at the light source PETRAIII at DESY, a member of the Helmholtz Association (HGF). We would like to thank the P03 beamline staff for assistance and support in using the beamline. DSC measurements were conducted at the Polymer Composites Institute, Hamburg University of Technology.

REFERENCES

(1) Ghosh, V.; Ziegler, G. R.; Anantheswaran, R. C. Fat, Moisture, and Ethanol Migration through Chocolates and Confectionary Coatings. *Crit. Rev. Food Sci. Nutr.* **2002**, *42*, 583−626.

(2) Aguilera, J. M.; Michel, M.; Mayor, G. Fat Migration in Chocolate: Diffusion or Capillary Flow in a Particulate Solid?—A Hypothesis Paper. *J. Food Sci.* **2004**, *69*, 167−174.

(3) Choi, Y. J.; McCarthy, K. L.; McCarthy, M. J.; Kim, M. H. Oil Migration in Chocolate. *Appl. Magn. Reson.* **2007**, *32*, 205−220.

(4) Lonchampt, P.; Hartel, R. W. Fat Bloom in Chocolate and Compound Coatings. *Eur. J. Lipid Sci. Technol.* **2004**, *106*, 241−274.

(5) Walter, P.; Cornillon, P. Lipid Migration in Two-Phase Chocolate Systems Investigated by NMR and DSC. *Food Res. Int.* **2002**, *35*, 761−767.

(6) Galdámez, J. R.; Szlachetka, K.; Duda, J. L.; Ziegler, G. R. Oil Migration in Chocolate: A Case of Non-Fickian Diffusion. *J. Food Eng.* **2009**, *92*, 261−268.

(7) Rousseau, D.; Smith, P. Microstructure of Fat Bloom Development in Plain and Filled Chocolate Confections. *Soft Matter* **2008**, *4*, 1706−1712.

(8) Loisel, C.; Keller, G.; Lecq, G.; Bourgaux, C.; Ollivon, M. Phase Transitions and Polymorphism of Cocoa Butter. *J. Am. Oil Chem. Soc.* **1998**, *75*, 425−429.

(9) Leventis, N.; Chidambareswarapattar, C.; Bang, A.; Sotiriou-Leventis, C. Cocoon-in-Web-Like Superhydrophobic Aerogels from Hydrophilic Polyurea and Use in Environmental Remediation. *ACS Appl. Mater. Interfaces* **2014**, *6*, 6872−6882.

(10) Maleky, F.; McCarthy, K. L.; McCarthy, M. J.; Maragoni, A. G. Effect of Cocoa Butter Structure on Oil Migration. *J. Food Sci.* **2012**, *77*, E74−E79.

(11) Tabouret, T. Technical Note: Detection of Fat Migration in a Confectionery Product. *Int. J. Food Sci. Technol.* **1987**, *22*, 163−167.

(12) Strixner, T.; Sterr, J.; Kulozik, U.; Gebhardt, R. Structural Study on Hen-Egg Yolk High Density Lipoprotein (HDL) Granules. *Food Biophys.* **2014**, *9*, 314−321.

(13) Gebhardt, R.; Burghammer, M.; Riekel, C.; Kulozik, U.; Müller-Buschbaum, P. Investigation of Surface Modification of Casein Films by Rennin Enzyme Action using Micro-beam Grazing Incidence Small Angle X-Ray Scattering. *Dairy Sci. Technol.* **2010**, *90*, 75−86.

(14) Stalder, A. F.; Melchior, T.; Müller, M.; Sage, D.; Blu, T.; Unser, M. Low-Bond Axisymmetric Drop Shape Analysis for Surface Tension and Contact Angle Measurements of Sessile Drops. *Colloids Surf., A* **2010**, *364*, 72−81.

(15) Buffet, A.; Rothkirch, A.; Döhrmann, R.; Körstgens, V.; Abul Kashem, M.; Perlich, J.; Herzog, G.; Schwartzkopf, M.; Gehrke, R.; Müller-Buschbaum, P.; Roth, S. V. P03, the Microfocus and Nanofocus X-Ray Scattering (MiNaXS) Beamline of the PETRA III Storage Ring: The Microfocus Endstation. *J. Synchrotron Radiat.* **2012**, 647−653.

(16) Roth, S. V.; Herzog, G.; Körstgens, V.; Buffet, A.; Schwartzkopf, M.; Perlich, J.; Abul Kashem, M. M.; Döhrmann, R.; Gehrke, R.; Rothkirch, A.; Stassig, K.; Wurthm, W.; Benecke, G.; Li, C.; Fratzl, P.; Rawolle, M.; Müller-Buschbaum, P. In Situ Observation of Cluster Formation during Nanoparticle Solution Casting on a Colloidal Film. *J. Phys.: Condens. Matter* **2011**, *23*, 254208.

(17) Santoro, G.; Buffet, A.; Döhrmann, R.; Yu, S.; Körstgens, V.; Müller-Buschbaum, P.; Gedde, U.; Hedenqvist, M.; Roth, S. V. Use of Intermediate Focus for Grazing Incidence Small and Wide Angle X-Ray Scattering Experiments at the Beamline P03 of PETRA III, DESY. *Rev. Sci. Instrum.* **2014**, *85*, 043901−1−043901−9.

(18) Benecke, G.; Wagermaier, W.; Li, C.; Schwartzkopf, M.; Flucke, G.; Hoerth, R.; Zizak, I.; Burghammer, M.; Metwalli, E.; Müller-Buschbaum, P.; Trebbin, M.; Förster, S.; Paris, O.; Roth, S. V.; Fratzl, P. A Customizable Software for Fast Reduction and Analysis of Large X-Ray Scattering Data Sets: Applications of the New DPDAK Package to Small-Angle X-Ray Scattering and Grazing-Incidence Small-Angle X-Ray Scattering. *J. Appl. Crystallogr.* **2014**, *47*, 1797−1803.

(19) Porod, G. Chapter 2: General Theory. *Small Angle X-Ray Scattering*. Glatter, O., Kratky, O., Eds. Academic Press: New York, 1982, 17−51.

(20) Wille, R. L.; Lutton, E. S. Polymorphism of Cocoa Butter. *J. Am. Oil Chem. Soc.* **1966**, *43*, 491−496.

(21) Chapman, G. M.; Akehurst, E. E.; Wright, W. B. Cocoa Butter and Confectionery Fats. Studies Using Programmed Temperature X-Ray Diffraction and Differential Scanning Calorimetry. *J. Am. Oil Chem. Soc.* **1971**, *48*, 824−830.

(22) Gebhardt, R.; Roth, S. V.; Burghammer, M.; Riekel, C.; Tolkach, A.; Kulozik, U.; Müller-Buschbaum, P. Structural Changes of Casein Micelles in a Rennin Gradient Film with Simultaneous Consideration of the Film Morphology. *Int. Dairy J.* **2010**, *20*, 203−211.

(23) Gebhardt, R.; Vendrely, C.; Kulozik, U. Structural Characterization of Casein Micelles: Shape Changes during Film Formation. *J. Phys.: Condens. Matter* **2011**, *23*, 444201.

(24) Holt, C.; de Kruif, C. G.; Tuinier, R.; Timmins, P. A. Substructure of Bovine Casein Micelles by Small-Angle X-Ray and Neutron Scattering. *Colloids Surf., A* **2003**, *213*, 275−284.

DOI: 10.1021/acsami.5b02092
ACS Appl. Mater. Interfaces 2015, 7, 9929−9936

(25) Shukla, A.; Theyencheri, N.; Zanchi, D. Structure of Casein Micelles and their Complexation with Tannins. *Soft Matter* **2009**, *5*, 2884−2888.
(26) McMahon, D. J.; Oommen, B. S. Supramolecular Structure of the Casein Micelle. *J. Dairy Sci.* **2008**, *91*, 1709−1721.
(27) Gebhardt, R.; Burghammer, M.; Riekel, C.; Roth, S. V.; Müller-Buschbaum, P. Structural Changes of Casein Micelles in a Calcium Gradient Film. *Macromol. Biosci.* **2008**, *8*, 347−54.
(28) Metin, S.; Hartel, R. W. Chapter 2: Crystallization of Fats and Oils.*Bailey's Industrial Oil and Fat Products*. 6th ed. Shahidi, F., Ed. John Wiley & Sons, Inc.: Hoboken, NJ, 2005.
(29) Saha, D.; Payzant, E. A.; Kumbhar, A. S.; Naskar, A. K. Sustainable Mesoporous Carbons as Storage and Controlled-Delivery Media for Functional Molecules. *ACS Appl. Mater. Interfaces* **2013**, *5*, 5868−5874.
(30) Zeng, Y.; Braun, P.; Windhab, E. Tempering, Continuous Precrystallization of Chocolate with Seed Cocoa Butter Crystal Suspension. *Manuf. Confect.* **2002**, *4*, 71−80.
(31) Smith, K. W.; Cain, F. W.; Talbot, G. Effect of Nut Oil Migration on Polymorphic Transformation in a Model System. *Food Chem.* **2007**, *102*, 656−663.
(32) Lee, W. L.; McCarthy, M. J.; McCarthy, K. L. Oil Migration in 2-Component Confectionery Systems. *J. Food Sci.* **2009**, *75*, 1750−3841.
(33) Li, W.; Wu, Y.; Liang, W.; Li, B.; Liu, S. Reduction of the Water Wettability of Cellulose Film through Controlled Heterogeneous Modification. *ACS Appl. Mater. Interfaces* **2014**, *6*, 5726−5734.

DOI: 10.1021/acsami.5b02092
ACS Appl. Mater. Interfaces 2015, 7, 9929−9936